

Anticrossings in Förster Coupled Quantum Dots

Ahsan Nazir, Brendon W. Lovett, Sean D. Barrett, John H. Reina, and G. Andrew D. Briggs

Abstract—We consider two coupled generic quantum dots, each modelled by a simple potential which is given by infinite parabolic potential wells in all three (x -, y -, z -) dimensions. This potential profile allows the derivation of an analytical expression for the inter-dot Förster coupling, in the dipole-dipole approximation. We investigate the energy level behaviour of this coupled two-dot system under the influence of an external applied electric field and predict the presence of anticrossings in the optical spectra due to the Förster interaction.

Index Terms—Excitons, Quantum Dots, Quantum Computation, Anticrossings, Resonant Energy Transfer

I. INTRODUCTION

EXCITONS (electron-hole bound states) within quantum dots have already attracted much interest in the field of quantum computation and have formed the basis of several proposals for quantum logic gates. For example in Ref. [1], the energy shift due to the exciton-exciton dipole interaction between two quantum dots is considered. This interaction gives rise to diagonal terms in the interaction Hamiltonian and hence it is proposed that quantum logic may be performed via ultra-fast laser pulses. However, excitons within adjacent quantum dots are also able to interact through their resonant (Förster) energy transfer [2], some evidence for which has been obtained experimentally in a range of systems [3], [4], [5], [6]. As is shown below, this resonant transfer of energy gives rise to off-diagonal Hamiltonian matrix elements and therefore to a naturally entangling quantum evolution. It is proposed here that this interaction may be observed in a straightforward way, through the observation of anticrossings induced in the coupled dot energy spectra by the application of an external static electric field. We also show that the off-diagonal matrix elements can be made sufficiently large to be of interest for excitonic quantum computation [7].

The first studies of Förster resonant energy transfer were performed in the context of the sensitized luminescence of solids [2], [8]. Here, an excited sensitizer atom can transfer its excitation to a neighbouring acceptor atom, via an intermediate virtual photon. This same mechanism has also been shown to be responsible for exciton transfer between quantum dots [4], and within molecular systems [5] and biosystems [6] (as a mechanism for photosynthesis), all of which may be treated

This work has been submitted to the IEEE for possible publication. Copyright may be transferred without notice, after which this version may no longer be accessible.

A. Nazir, B. W. Lovett, and G. A. D. Briggs are with the Department of Materials, Oxford University, Oxford OX1 3PH, U. K. (email: ahsan.nazir@materials.ox.ac.uk).

S. D. Barrett is with Hewlett-Packard Laboratories, Filton Road, Stoke Gifford, Bristol BS34 8QZ, U. K.

J. H. Reina is with the Department of Materials, Oxford University, Oxford OX1 3PH, U. K., and the Clarendon Laboratory, Department of Physics, Oxford University, Oxford OX1 3PU, U.K., and on leave from Centro Internacional de Física (CIF), A.A. 4948, Bogotá, Colombia.

in a similar formulation. Thus, the results reported here can be expected to apply not only to quantum dot systems, but also to a wide range of nanostructures where Förster processes are of primary significance.

In this paper, we consider two coupled generic quantum dots, each modelled by a simple potential which is given by infinite parabolic wells in all three (x -, y -, z -) dimensions. This potential profile allows an analytical expression for the inter-dot Förster coupling in the dipole-dipole approximation to be derived and, although it only allows for qualitative predictions about real observations, it has been widely used in the literature [1], [9], [10], [11]. Excitations of each dot are assumed to be produced optically and we neglect tunnelling effects between the two coupled dots. We shall consider only the ground state (no exciton) and first excited state (one exciton) within our model, and these two states define our qubit basis as $|0\rangle$ and $|1\rangle$ respectively.

Various techniques exist for growing quantum dots in the laboratory, of which the Stranski-Krastanow method [12], [13] is possibly the most promising for the realization of a controllably coupled many dot system. In this growth mode a semiconductor is grown on a substrate which is made of a different semiconductor, leading to a lattice mismatch between the layers. Under certain growth conditions, dots form spontaneously due to the competing energy considerations of dot surface area, strain, and volume. Interestingly, if a spacer layer of material is then grown above the first dot layer, and then a second dot layer deposited, a vertically correlated arrangement of dots can be made [14]. Two such stacked dots could then form our interacting two qubit system with materials, growth conditions, and spacer layer size tailored to give suitable electronic properties and inter-dot Coulomb interactions.

II. THE QUANTUM DOT MODEL

A. Single Particle States

Many varying approaches to the calculation of electron and hole states in quantum dots have been put forward in Refs. [9], [10], [15], [16], [17], [18], the choice of which depends on the final aim of the work. The aim here is to provide a simple illustration of how to observe resonant energy transfer between quantum dots experimentally, and how to exploit this inter-dot interaction to perform quantum logic. Therefore, we shall consider the most basic models [1], [9], [10] that can provide us with analytical expressions for the energies of the single particle states and for the dipole-dipole interaction between two dots.

In the effective mass and envelope function approximations [19], [20] the Schrödinger equation for single particles

may be written as:

$$H_i(\mathbf{r})\phi_i(\mathbf{r}) = \left[-\frac{\hbar^2}{2} \nabla \left(\frac{1}{m_i^*} \right) \nabla + V_i(\mathbf{r}) \right] \phi_i(\mathbf{r}) = E_i \phi_i(\mathbf{r}), \quad (1)$$

where $i = e, h$ for electron or hole, $V_i(\mathbf{r})$ is the dot confinement potential which accounts for the difference in band-gaps across the heterostructure, and m_i^* is the effective mass of particle i . Here, $\phi_i(\mathbf{r})$ is the envelope function part of the total wavefunction:

$$\psi_i(\mathbf{r}) = \phi_i(\mathbf{r})U_i(\mathbf{r}). \quad (2)$$

The envelope function describes the slowly varying contribution to the change in wavefunction amplitude over the dot region and the physical properties of the single particle states can be derived purely from this contribution. $U_i(\mathbf{r})$ is called the Bloch function and has the periodicity of the atomic lattice. Its consideration is vital when describing the interactions between two or more particles.

In the simple analytical model, a separable potential comprising infinite parabolic wells in all three dimensions represents the quantum dot:¹

$$V(x, y, z) = \frac{1}{2}c_{i,x}x^2 + \frac{1}{2}c_{i,y}y^2 + \frac{1}{2}c_{i,z}z^2, \quad (3)$$

where the frequency $\omega_{i,j} = \sqrt{c_{i,j}/m^*}$ for $j = x, y, z$. Hence, the Schrödinger equation (1) is also separable and provides simple product solutions for the electron and hole states. The envelope functions are therefore given by:

$$\phi_i(\mathbf{r}) = \xi_{i,x}(x)\xi_{i,y}(y)\xi_{i,z}(z), \quad (4)$$

for the parabolic confinement ($\mathbf{r} = (x, y, z)$). We now drop the subscript i but remember that due to their differing effective masses electrons and holes may take different values for the constants defined throughout this paper.

The solutions to the one-dimensional Schrödinger equation for the potential form (3) are given by:

$$\xi^n(x) = \left(\frac{1}{n!2^n d_x \sqrt{\pi}} \right)^{1/2} H_n \left(\frac{x}{d_x} \right) \exp \left(-\frac{x^2}{2d_x^2} \right), \quad (5)$$

in the x - direction with analogous expressions for y and z . The constant $n = (0, 1, 2, 3, \dots)$ labels the quantum state, with energy $E_n = (n + 1/2)\hbar\omega_x$, the H_n 's are Hermite polynomials, and $d_x = (\hbar/\sqrt{m^*c_x})^{1/2} = (\hbar/(m^*\omega_x))^{1/2}$. We are only interested in the ground state solutions of each well so our envelope function is given by:

$$\begin{aligned} \phi(x, y, z) &= \left(\frac{1}{d_x d_y d_z \pi^{3/2}} \right)^{1/2} \exp \left(-\frac{x^2}{2d_x^2} \right) \\ &\times \exp \left(-\frac{y^2}{2d_y^2} \right) \exp \left(-\frac{z^2}{2d_z^2} \right), \quad (6) \end{aligned}$$

with energy $E_0 = \frac{1}{2}\hbar(\omega_x + \omega_y + \omega_z)$. The choice of constants c_j and hence d_j will be different for changing confinement potentials and particle masses, and so will depend upon the

¹With this choice of potential we are able to model both the convenient situation of a spherically symmetric quantum dot, and the more common situation in self-assembled dots of stronger confinement in the growth (z) direction than in the x, y plane.

energies of the system under consideration and whether the particle is an electron or hole.

B. Excitons and Coulomb Integrals

The excitation of an electron from a valence band state to a conduction band state leaves a hole in the valence band. The electron and hole are oppositely charged and may form a bound state, the exciton, and as stated earlier we consider the absence or presence of a ground state exciton within a dot to form our qubit basis ($|0\rangle$ and $|1\rangle$ respectively). Therefore, for excitons, we must consider an electron-hole pair Hamiltonian:

$$H = H_e + H_h - \frac{e^2}{4\pi\epsilon(\mathbf{r}_e - \mathbf{r}_h)|\mathbf{r}_e - \mathbf{r}_h|} + E^{gap}, \quad (7)$$

where H_e and H_h are given by (1) with the appropriate effective masses and potentials; E^{gap} is the semiconductor band-gap energy, and $\epsilon(\mathbf{r}_e - \mathbf{r}_h)$ is the background dielectric constant of the semiconductor. We shall consider the simplest case of $\epsilon(\mathbf{r}_e - \mathbf{r}_h) = \epsilon_0\epsilon_r$, i.e. the relative permittivity ϵ_r is independent of $(\mathbf{r}_e - \mathbf{r}_h)$. The intra-dot energy shift due to the Coulomb term $H_{eh} = e^2/4\pi\epsilon_0\epsilon_r|\mathbf{r}_e - \mathbf{r}_h|$ is a small contribution to the total energy and we treat it as a first-order perturbation.

We construct an antisymmetric wavefunction representing a single exciton state given by:

$$\Psi_I = A [\psi'_n(\mathbf{r}_1, \sigma_1), \psi_m(\mathbf{r}_2, \sigma_2)], \quad (8)$$

where \mathbf{r} and σ are position (from the centre of the dot) and spin variables respectively, n and m label the quantum states, and A denotes overall antisymmetry. Here, one electron $\psi'_n(\mathbf{r}_1, \sigma_1)$ has been promoted from the valence band into a conduction band state whilst $\psi_m(\mathbf{r}_2, \sigma_2)$ represents a state in the valence band. Taking the Coulomb matrix element between the initial state Ψ_I above and an identical state Ψ_F (in effect coupling an electron and hole via the Coulomb operator) leads to two terms [21], [22], the direct term:

$$\begin{aligned} M_{IF}^{Direct} &= \frac{e^2}{4\pi\epsilon_0\epsilon_r} \int \int \psi_n'^*(\mathbf{r}_1) \psi_n'(\mathbf{r}_1) \frac{1}{|\mathbf{r}_1 - \mathbf{r}_2|} \\ &\times \psi_m^*(\mathbf{r}_2) \psi_m(\mathbf{r}_2) d\mathbf{r}_1 d\mathbf{r}_2, \quad (9) \end{aligned}$$

and the exchange term:

$$\begin{aligned} M_{IF}^{Exch} &= \pm \frac{e^2}{4\pi\epsilon_0\epsilon_r} \int \int \psi_n'^*(\mathbf{r}_1) \psi_m(\mathbf{r}_1) \frac{1}{|\mathbf{r}_1 - \mathbf{r}_2|} \\ &\times \psi_n'(\mathbf{r}_2) \psi_m^*(\mathbf{r}_2) d\mathbf{r}_1 d\mathbf{r}_2. \quad (10) \end{aligned}$$

The sign of the exchange term is determined by the symmetry of the spin state of the two particles; triplet spin states give positive exchange elements whereas singlet spin states give negative values. We shall now show how to calculate the direct electron-hole Coulomb matrix element on a single dot where n and m are both taken as ground states. The exchange interaction is much smaller [21] and we shall not consider it here.

If we consider identical potential wells in all three directions then we can use the spherical symmetry of the system to derive an analytical expression for the direct Coulomb matrix element which we call M_{eh} . For identical wells in all three dimensions

($d_x = d_y = d_z = d$), (6) may be written in spherical polar coordinates as:

$$\phi(\mathbf{r}) = \left(\frac{1}{d\sqrt{\pi}}\right)^{3/2} \exp\left(-\frac{r^2}{2d^2}\right). \quad (11)$$

Substituting into (9) leads to:

$$M_{eh} = \frac{e^2}{4\pi\epsilon_0\epsilon_r} \left(\frac{1}{d_e\sqrt{\pi}}\right)^3 \left(\frac{1}{d_h\sqrt{\pi}}\right)^3 \iint \exp\left(-\frac{r_1^2}{d_e^2}\right) \times \exp\left(-\frac{r_2^2}{d_h^2}\right) \frac{1}{|\mathbf{r}_1 - \mathbf{r}_2|} d\mathbf{r}_1 d\mathbf{r}_2, \quad (12)$$

where we have assumed that the contribution of the Bloch functions $U(\mathbf{r})$ may be neglected. We now express $1/|\mathbf{r}_1 - \mathbf{r}_2|$ in terms of Legendre polynomials as [23]:

$$\frac{1}{|\mathbf{r}_1 - \mathbf{r}_2|} = \begin{cases} \frac{1}{r_1} \sum_{l=0}^{\infty} \left(\frac{r_2}{r_1}\right)^l P_l(\cos\theta), & \text{for } r_1 > r_2 \\ \frac{1}{r_2} \sum_{l=0}^{\infty} \left(\frac{r_1}{r_2}\right)^l P_l(\cos\theta), & \text{for } r_1 < r_2. \end{cases} \quad (13)$$

Substituting this into (12) and integrating over polar angles leads to:

$$M_{eh} = \frac{4\pi e^2}{\epsilon_0\epsilon_r} \left(\frac{1}{d_e\sqrt{\pi}}\right)^3 \left(\frac{1}{d_h\sqrt{\pi}}\right)^3 \int_0^{\infty} \exp\left(-\frac{r_1^2}{d_e^2}\right) r_1^2 dr_1 \times \left\{ \int_0^{r_1} \frac{1}{r_1} \exp\left(-\frac{r_2^2}{d_h^2}\right) r_2^2 dr_2 + \int_{r_1}^{\infty} \frac{1}{r_2} \exp\left(-\frac{r_2^2}{d_h^2}\right) r_2^2 dr_2 \right\}, \quad (14)$$

where use has been made of the orthogonality relations of Legendre polynomials. The integrations are now simple and give us the following expression for M_{eh} :

$$M_{eh} = \frac{1}{2} \frac{e^2}{\pi^{3/2}\epsilon_0\epsilon_r} \frac{1}{\sqrt{d_e^2 + d_h^2}}. \quad (15)$$

In a similar manner, we may also approximate the behaviour of M_{eh} in the presence of an external electric field. For a constant field applied to the dot, the potential in the field direction (for simplicity say z , although the spherical symmetry we assume means all three directions are equivalent) becomes:

$$V(z) \mapsto V(z) + qFz, \quad (16)$$

Where $q = -e$ for conduction band electrons, $q = +e$ for holes, and F is the electric field strength. Substituting this into the Schrödinger equation for the z -component leads us to a new Schrödinger equation that has the same parabolic potential form:

$$\left[-\frac{\hbar^2}{2m^*} \frac{\partial^2}{\partial z'^2} + \frac{1}{2} c_z z'^2\right] \phi(z') = E' \phi(z') \quad (17)$$

with

$$\begin{aligned} z'_e &= z - eF/c_{e,z} && \text{for electrons,} \\ z'_h &= z + eF/c_{h,z} && \text{for holes,} \\ E'_i &= E + (eF)^2/2c_{i,z} && i = e, h. \end{aligned} \quad (18)$$

Therefore, electrons and holes are displaced in opposite directions and their envelope functions are the same as (6) with

z replaced by z' . The simplicity of the change in envelope function with applied electric field is a great advantage of the parabolic well model, although it should be pointed out that this same simplicity implies that the charges can continue separating indefinitely with applied field strength and is therefore unrealistic at very high fields.

Again, in spherical polar coordinates, the envelope functions in the presence of a field may be written as:

$$\phi_e(\mathbf{r}) = \left(\frac{1}{d_e\sqrt{\pi}}\right)^{3/2} \exp\left(-\frac{(\mathbf{r} - \hat{\mathbf{k}}eF/c_e)^2}{2d_e^2}\right) \quad (19)$$

for electrons, and:

$$\phi_h(\mathbf{r}) = \left(\frac{1}{d_h\sqrt{\pi}}\right)^{3/2} \exp\left(-\frac{(\mathbf{r} + \hat{\mathbf{k}}eF/c_h)^2}{2d_h^2}\right) \quad (20)$$

for holes, where $\hat{\mathbf{k}}$ is the unit vector in the z -direction. This time, substituting into (9) leads to:

$$M_{eh} = C \iint \exp\left(-\frac{r_1^2}{d_e^2}\right) \exp\left(-\frac{r_2^2}{d_h^2}\right) \times \exp(r_1\alpha \cos\theta) \frac{1}{|\mathbf{r}_1 - \mathbf{r}_2|} d\mathbf{r}_1 d\mathbf{r}_2, \quad (21)$$

where

$$C = \frac{e^2}{4\pi\epsilon_0\epsilon_r} \left(\frac{1}{d_e\sqrt{\pi}}\right)^3 \left(\frac{1}{d_h\sqrt{\pi}}\right)^3 \times \exp\left[-\frac{(eF)^2}{d_e^2} \left(\frac{1}{c_e} + \frac{1}{c_h}\right)^2\right], \quad (22)$$

and

$$\alpha = \frac{2eF}{d_e^2} \left(\frac{1}{c_e} + \frac{1}{c_h}\right). \quad (23)$$

We proceed as before, again making use of Legendre polynomials and their orthogonality relations, and integrate over \mathbf{r}_2 to leave

$$M_{eh} = \frac{2\pi^{5/2} C d_h^3}{\alpha} \int \exp\left(-\frac{r_1^2}{d_e^2}\right) \operatorname{erf}\left(\frac{r_1}{d_h}\right) \times [\exp(r_1\alpha) - \exp(-r_1\alpha)] dr_1. \quad (24)$$

For $\alpha < 1/d_e$ (valid up to fields of order 10^7 V/m for $c_e = c_h = 0.00641$ J/m², $d_e = 2.627 \times 10^{-9}$ m), we expand the exponentials in α up to the term in α^3 and integrate over r_1 . Keeping only the terms up to F^2 order in the resultant expressions gives us an estimate for the suppression of the electron-hole binding energy as an external field is applied:

$$M_{eh} = \frac{e^2}{2\pi^{3/2}\epsilon_0\epsilon_r \sqrt{d_e^2 + d_h^2}} \times \left[1 - \frac{e^2 F^2}{3(d_e^2 + d_h^2)} \left(\frac{1}{c_e} + \frac{1}{c_h}\right)^2\right], \quad (25)$$

which reduces to (15) at $F = 0$.

III. A SIGNATURE OF FÖRSTER COUPLED QUANTUM DOTS

A. The Hamiltonian

We have now characterized the single particle electron and hole states within a simple quantum dot model, as well as accounting for the binding energy due to electron-hole coupling within a dot when estimating the ground state exciton energy. In this section we shall consider excitons in two coupled quantum dots and the Coulomb interactions between them. More specifically, we shall derive an analytical expression for the strength of the inter-dot Förster coupling. We shall show that this coupling is, under certain conditions, of dipole-dipole type [2], [8] and that it is responsible for resonant exciton exchange between adjacent quantum dots. This is a transfer of energy only, not a tunnelling effect.²

Following Ref. [7] we write the Hamiltonian of two interacting quantum dots in the computational basis $\{|00\rangle, |01\rangle, |10\rangle, |11\rangle\}$ as ($\hbar = 1$):

$$\hat{H} = \begin{pmatrix} \omega_0 & 0 & 0 & 0 \\ 0 & \omega_0 + \omega_2 & V_F & 0 \\ 0 & V_F & \omega_0 + \omega_1 & 0 \\ 0 & 0 & 0 & \omega_0 + \omega_1 + \omega_2 + V_{XX} \end{pmatrix} \quad (26)$$

where the off-diagonal Förster interaction is given by V_F , and the direct Coulomb binding energy between the two excitons, one on each dot, is on the diagonal and given by V_{XX} [1], [21]. The ground state energy is denoted by ω_0 , and $\Delta\omega \equiv \omega_1 - \omega_2$ is the difference between the excitation energy for dot I and that for dot II. The energies and eigenstates of this four-level system are given by:

$$\begin{aligned} E_{00} &= \omega_0, & |\Psi_{00}\rangle &= |00\rangle \\ E_- &= \omega_0 + \omega_1 - \frac{\Delta\omega}{2}(1+A), & |\Psi_-\rangle &= a_1|10\rangle - a_2|01\rangle \\ E_+ &= \omega_0 + \omega_1 - \frac{\Delta\omega}{2}(1-A), & |\Psi_+\rangle &= a_1|01\rangle + a_2|10\rangle \\ E_{11} &= \omega_0 + \omega_1 + \omega_2 + V_{XX}, & |\Psi_{11}\rangle &= |11\rangle, \end{aligned} \quad (27)$$

where $A = \sqrt{1 + 4(V_F/\Delta\omega)^2}$, $a_1 = \sqrt{(A-1)/2A}$, and $a_2 = \text{sgn}(V_F\Delta\omega)\sqrt{(A+1)/2A}$ for $|\Delta\omega| > 0$. We can see that V_F may cause a mixing of the states $|01\rangle$ and $|10\rangle$ with the result that $|\Psi_-\rangle$ and $|\Psi_+\rangle$ can now be entangled states. It is straightforward to see that an off-diagonal Förster coupling does indeed correspond to a resonant transfer of energy; if we begin in the state $|10\rangle$ (exciton on dot I, no exciton on dot II) this will naturally evolve to a state $|01\rangle$ (no exciton on dot I, exciton on dot II), in a time given by $\pi/(2V_F)$, through the maximally entangled state $2^{-1/2}(|10\rangle + i|01\rangle)$. An analogous behaviour is expected for the initial state $|01\rangle$.

B. Analytical Models of the Förster Interaction

We shall now calculate the magnitude of the off-diagonal matrix elements in (26) for the parabolic potential model. We shall see that the behaviour of the Förster interaction due to changes in dot size, composition, separation, and applied electric fields may be predicted by such an analytical model.

²If the electron and hole are strongly bound, so that they do not tunnel separately, a tunnelling between the two dots will simply add a small correction to the off-diagonal elements in the interaction Hamiltonian.

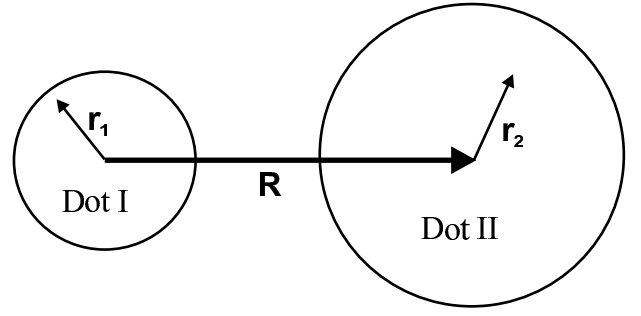


Fig. 1. Schematic diagram of the interacting two-dot system.

We begin by calculating the form of the matrix element in the dipole-dipole approximation.

The matrix element we require is that of the Coulomb operator between two single exciton wavefunctions, one located on each of the two dots. We take our initial state as representing a conduction band state in dot I, and a valence band state in dot II:

$$\Psi_I = A [\psi'_n(\mathbf{r}_1, \sigma_1), \psi_m(\mathbf{r}_2, \sigma_2)]. \quad (28)$$

For our final state, we must have a valence band state in dot I and a conduction band state in dot II, given by:

$$\Psi_F = A [\psi_n(\mathbf{r}_1, \sigma_1), \psi'_m(\mathbf{r}_2, \sigma_2)]. \quad (29)$$

The positions \mathbf{r}_1 and \mathbf{r}_2 are now defined from the centres of dot I and dot II respectively (see Fig. 1), and not from the same point as in (8) where only a single dot was considered. Note that the time ordering of Ψ_I and Ψ_F is irrelevant since, as described in Section III-A, the resonant energy transfer process is reversible.

Therefore, the direct Coulomb matrix element between these two states gives us

$$V_F = -\frac{e^2}{4\pi\epsilon_0\epsilon_r} \int \int \psi_n'^*(\mathbf{r}_1) \psi_n(\mathbf{r}_1) \frac{1}{|\mathbf{R} + \mathbf{r}_1 - \mathbf{r}_2|} \times \psi_m^*(\mathbf{r}_2) \psi_m'(\mathbf{r}_2) d\mathbf{r}_1 d\mathbf{r}_2, \quad (30)$$

where we have explicitly included the inter-dot separation \mathbf{R} . For $|\mathbf{R}| \gg |\mathbf{r}_1 - \mathbf{r}_2|$, which is valid so long as the characteristic sizes of the wavefunctions, d_j , are small in comparison to $|\mathbf{R}|$, we can follow the procedure of Dexter [8] and expand the Coulomb operator in powers of $(\mathbf{r}_{1/2}/\mathbf{R})$ up to second order. Taking the matrix element between Ψ_I and Ψ_F leads to:

$$V_F = -\frac{e^2}{4\pi\epsilon_0\epsilon_r R^3} \left[\langle \mathbf{r}_I \rangle \cdot \langle \mathbf{r}_{II} \rangle - \frac{3}{R^2} (\langle \mathbf{r}_I \rangle \cdot \mathbf{R}) (\langle \mathbf{r}_{II} \rangle \cdot \mathbf{R}) \right]. \quad (31)$$

We assume the dots are sufficiently separated for there to be no overlap of envelope functions between dot I and dot II. Therefore, we do not consider the exchange term of this Coulomb interaction. The integrals:

$$\langle \mathbf{r}_I \rangle = \int \psi_n'^*(\mathbf{r}_1) \mathbf{r}_1 \psi_n(\mathbf{r}_1) d\mathbf{r}_1, \quad (32)$$

$$\langle \mathbf{r}_{II} \rangle = \int \psi_m^*(\mathbf{r}_2) \mathbf{r}_2 \psi_m'(\mathbf{r}_2) d\mathbf{r}_2,$$

are taken between an electron and hole ground state centered on dot I and dot II respectively. Remembering that our wavefunctions are a product of an envelope function $\phi(\mathbf{r})$ and

a Bloch function $U(\mathbf{r})$ we can make use of their different periodicities to write [21]:

$$V_F = -\frac{1}{4\pi\epsilon_0\epsilon_r R^3} O_I O_{II} \left[\mathbf{d}_{cv(I)} \cdot \mathbf{d}_{cv(II)} - \frac{3}{R^2} (\mathbf{d}_{cv(I)} \cdot \mathbf{R})(\mathbf{d}_{cv(II)} \cdot \mathbf{R}) \right]. \quad (33)$$

The overlap integrals are defined as:

$$O = \int_{space} \phi_e(\mathbf{r}) \phi_h(\mathbf{r}) d\mathbf{r}, \quad (34)$$

with $O_{I/II}$ referring to the overlap of the envelope functions for dot I or dot II respectively (each having a maximum value of unity), and the inter-band dipole matrix elements are defined as:

$$\mathbf{d}_{cv} = e \int_{cell} U_e(\mathbf{r}) \mathbf{r} U_h(\mathbf{r}) d\mathbf{r}, \quad (35)$$

with $\mathbf{d}_{cv(I/II)}$ referring to the transition dipole for dot I or dot II respectively.

We shall not calculate the values of \mathbf{d}_{cv} here as they are commonly measured experimental quantities (see also Ref. [21] for a simple model) and, once the dot materials have been chosen, are constant contributions to the Förster interaction strength. However, the calculation of $O_{I/II}$ is vital in determining the effects of dot size, shape, and applied electric fields on the strength of the inter-dot interaction.

We take the parabolic solutions in Cartesian coordinates from (6) and also include the effect of a lateral electric field, which is important in determining how to suppress the interaction when required, or bring two non-identical dots into resonance. As before, we shall assume that the electric field only affects the envelope function part of the wavefunction; this is valid in the regime where the electric field never becomes so large that the envelope function varies on the unit cell scale. This is equivalent to saying that the envelope functions can be decomposed into a superposition of crystal momentum (\mathbf{k}) eigenstates near the band edges, where the Bloch functions are approximately independent of \mathbf{k} .

For a constant field in the lateral direction (say x) the overlap integrals $O_{I/II}$ are straightforward to calculate. Again, for clarity, we take identical wells in all three directions for both electrons and holes ($d_x = d_y = d_z = d$), leading to

$$\begin{aligned} \phi_e(\mathbf{r}) &= \left(\frac{1}{d_e \sqrt{\pi}} \right)^{3/2} \exp \left(-\frac{(x - eF/c_e)^2}{2d_e^2} \right) \\ &\times \exp \left(-\frac{(y^2 + z^2)}{2d_e^2} \right), \end{aligned} \quad (36)$$

for electrons, and

$$\begin{aligned} \phi_h(\mathbf{r}) &= \left(\frac{1}{d_h \sqrt{\pi}} \right)^{3/2} \exp \left(-\frac{(x + eF/c_h)^2}{2d_h^2} \right) \\ &\times \exp \left(-\frac{(y^2 + z^2)}{2d_h^2} \right), \end{aligned} \quad (37)$$

for holes. Substituting into (34) and integrating results in

$$O = \left(\frac{2d_e d_h}{d_e^2 + d_h^2} \right)^{3/2} \exp \left\{ -\frac{e^2 F^2 (c_e + c_h)^2}{2c_e^2 c_h^2 (d_e^2 + d_h^2)} \right\}. \quad (38)$$

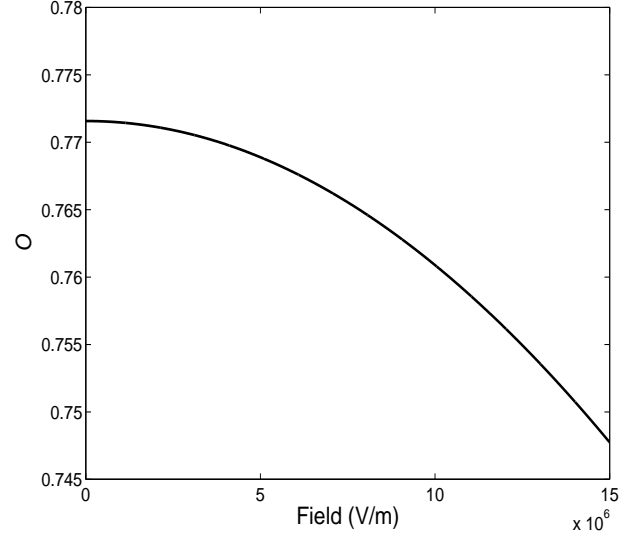


Fig. 2. Dependence of the overlap integral of a single parabolic quantum dot as a function of the in-plane (x -direction) electric field strength. Suppression of the Förster interaction results from the reduction in electron-hole overlap for increasing fields. A 500 meV potential at $x = 5$ nm from the dot centre for both electrons and holes is used, giving $c = 0.00641$ J/m².

Therefore, in zero applied field the overlap depends only on the ratio $(2d_e d_h / (d_e^2 + d_h^2))^{3/2}$. It is worth noting that if we had chosen an infinite square well potential in the growth (z) direction and parabolic wells in the x - and y -directions (as is common in the literature [9]) then the zero field value would be $(2d_e d_h / (d_e^2 + d_h^2))$ with the field dependence being exactly the same as in (38).

Fig. 2 shows the suppression of the overlap integrals by an in-plane electric field (x -direction) and therefore the suppression of the Förster interaction itself. However, as we shall see in the next section, this does not rule out its observation in coupled dot systems that are tuned into resonance with an external applied field. Indeed, if the inter-dot interaction matrix element is relatively large in zero applied field, then interesting anticrossing behaviour should be observed in the energy spectrum as the system is tuned through resonance. We also note that a suppressed Förster coupling can be of benefit to the exciton-exciton dipole interaction quantum computation schemes [1] as it ensures an almost purely diagonal interaction between adjacent quantum dots.

Taking measured values for the transition dipole moment \mathbf{d}_{cv} allows us to estimate the magnitude of V_F between two stacked dots. In CdSe quantum dots a value for \mathbf{d}_{cv} of up to 5.2 eÅ has been reported [4] whilst for both InGaAs/GaAs and InAs/InGaAs quantum dots values of approximately 5-7 eÅ have been measured [24], [25]. Considering (33) with a value of 6 eÅ for \mathbf{d}_{cv} , overlap integrals $O_I = O_{II} = 1$, $\epsilon_r = 12$ (for InGaAs/GaAs), and inter-dot spacing $R = 5$ nm, we obtain an estimate of 0.69 meV for the Förster coupling energy V_F , certainly large enough to be observed experimentally. This corresponds to a resonant energy transfer time of picosecond order and is therefore interesting as a coupling mechanism for performing quantum logic gates, as it is well within the

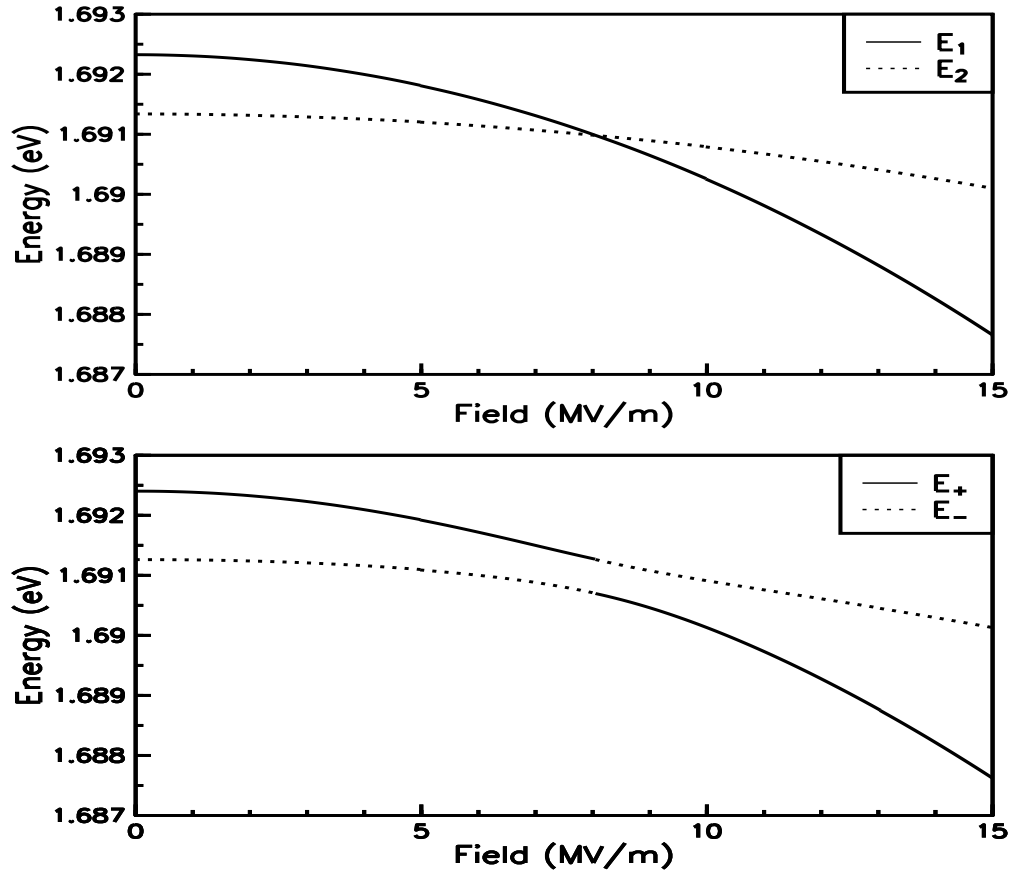


Fig. 3. (a) Single dot energies as a function of applied electric field. Parameters: $m_e^* = 0.04m_0$, $m_h^* = 0.45m_0$, $\epsilon_r = 12$, $c_I = 0.00641$ J/m² (corresponding to a potential of 500 meV at a distance of 5nm from the dot centre) for dot I, for both electrons and holes, and $c_{II} = 0.0256$ J/m² (corresponding to a potential of 500 meV at a distance of 2.5 nm from the dot centre) for dot II, for both electrons and holes. E^{gap} is taken as 1.2 eV for dot I and 0.681 eV for dot II. (b) Energies E_- and E_+ of the coupled dot system demonstrating anticrossing at a field of approximately 8×10^6 V/m. Here, V_F has a magnitude of 0.29 meV at zero field, with $d_{cv} = 5$ eÅ.

nanosecond dephasing times [26], [27], [28] expected for excitons within quantum dots (see Section IV for further discussion).

In the next section we shall discuss a signature of the Förster interaction that would be observable through photoluminescence measurements.

C. Anticrossings: A Signature of Förster Coupling

If we consider again (27) we can see that $|\Psi_-\rangle$ and $|\Psi_+\rangle$ have a range of forms depending upon the values of a_1 and a_2 . For example, if $\Delta\omega \gg V_F$, then $A \simeq 1$ which leads to $|a_1| \simeq 0$ and $|a_2| \simeq 1$. Therefore the states $|\Psi_-\rangle$ and $|\Psi_+\rangle$ are given by $|01\rangle$ and $|10\rangle$ respectively and there is no mixing of the computational basis states. The only way to couple two dots in this case is via the diagonal interaction V_{XX} . However, for two dots coupled by V_F at resonance ($\Delta\omega = 0$) we can see from (27) and by using $A = \sqrt{(\Delta\omega^2 + 4V_F^2)}/\Delta\omega^2$ that $|a_1| = |a_2| = 1/\sqrt{2}$, $E_{\text{lower}} = \omega_0 + \omega_1 - |V_F|$, and $E_{\text{higher}} = \omega_0 + \omega_1 + |V_F|$. Furthermore, the two eigenstates $2^{-1/2}(|01\rangle + |10\rangle)$ and $2^{-1/2}(|10\rangle - |01\rangle)$ are both maximally entangled and separated in energy by $2V_F$.

Interestingly, we should be able to move between these two cases by bringing two initially non-resonant coupled dots into resonance, for example by the application of a

static external electric field. By taking the dots through the resonance, an anticrossing of the energy levels should be observable through photoluminescence measurements. However, the transition from the antisymmetric state to the ground state is not dipole allowed on resonance and should also display a characteristic loss of intensity close to the resonant condition.

From (18) we see that an external field reduces the energy E for both electrons and holes, with the shift being greater for bigger dots. We therefore consider two coupled dots of similar material, with one of slightly greater dimensions and having a larger band-gap, and in Fig. 3(a) show that the single dot energy levels cross (for our choice of parameters) as an electric field is applied. Such a situation is plausible for systems such as InGaAs where dot layers of varying Indium content, and hence varying band-gap, may be grown [29] (see also Section IV below). Diagonalising the Hamiltonian (26) as the field strength F varies gives us a model prediction for the behaviour of the energy levels E_- and E_+ as shown in Fig. 3(b), where an anticrossing is observed at a field of approximately 8×10^6 V/m. Note that ω_1 , ω_2 , and V_F are all functions of F as shown in (18) and (38) respectively, which gives us a large scope for finding parameter regimes with interesting behaviour.

An analytical expression for the field strength at resonance

can be calculated from the condition $\Delta\omega = 0$. The total energy of each dot is given by:

$$E = E^{gap} + \frac{3\hbar}{2} \left(\sqrt{\frac{c}{m_e^*}} + \sqrt{\frac{c}{m_h^*}} \right) - \frac{(eF)^2}{c} - M_{eh}, \quad (39)$$

for identical potential wells in all directions for both electrons and holes ($c_x = c_y = c_z = c$). When dot I and dot II are resonant:

$$\begin{aligned} E_I - E_{II} &= 0 \\ &= (E_I^{gap} - E_{II}^{gap}) + \frac{3\hbar}{2} \left[\sqrt{c_I} \left(\frac{1}{\sqrt{m_e^*}} + \frac{1}{\sqrt{m_h^*}} \right) \right. \\ &\quad \left. - \sqrt{c_{II}} \left(\frac{1}{\sqrt{m_e^*}} + \frac{1}{\sqrt{m_h^*}} \right) \right] \\ &\quad - (eF)^2 \left(\frac{1}{c_I} - \frac{1}{c_{II}} \right) - M_{eh_I} + M_{eh_{II}}, \quad (40) \end{aligned}$$

therefore:

$$\begin{aligned} F^2 &= \frac{1}{\beta e^2} \left\{ (E_I^{gap} - E_{II}^{gap}) \right. \\ &\quad + \frac{3\hbar}{2} \left[(\sqrt{c_I} - \sqrt{c_{II}}) \left(\frac{1}{\sqrt{m_e^*}} + \frac{1}{\sqrt{m_h^*}} \right) \right] \\ &\quad \left. - \frac{e^2}{2\pi^{3/2}\epsilon_0\epsilon_r} \left[\frac{1}{(d_{eI}^2 + d_{hI}^2)^{1/2}} - \frac{1}{(d_{eII}^2 + d_{hII}^2)^{1/2}} \right] \right\}, \quad (41) \end{aligned}$$

where:

$$\begin{aligned} \beta &= \frac{1}{c_I} \left[1 - \frac{2e^2}{3\pi^{3/2}\epsilon_0\epsilon_r} \frac{1}{(d_{eI}^2 + d_{hI}^2)^{3/2}} \frac{1}{c_I} \right] \\ &\quad - \frac{1}{c_{II}} \left[1 - \frac{2e^2}{3\pi^{3/2}\epsilon_0\epsilon_r} \frac{1}{(d_{eII}^2 + d_{hII}^2)^{3/2}} \frac{1}{c_{II}} \right], \quad (42) \end{aligned}$$

and the states $|\Psi_-\rangle$ and $|\Psi_+\rangle$ should be maximally entangled at this value of F ($= 8.04 \times 10^6$ V/m with the same parameters as for Fig. 3), with an energy separation equal to $2V_F$ as stated earlier. Clearly, the anticrossing shown in Fig. 3(b) is an extremely strong indication of Förster coupling between the two dots, and also a first indication that entangled states are being produced.

IV. FURTHER WORK AND CONCLUSIONS

The experimental observation through photoluminescence of an anticrossing of the type above would be a tremendous result, and although it could be a difficult experiment to perform, it may well yield quicker results than attempting coherent control experiments on coupled dot systems. In future we intend to extend this work to include a study of the intensity of emitted light expected from the states $|\Psi_-\rangle$ and $|\Psi_+\rangle$ and the effects of the finite linewidth that would be observed due to T_1 (recombination) and T_2 (dephasing) processes.

The main question here is how feasible is it to bring two dots into resonance via a static external electric field. As has been mentioned above, and can be seen in Fig. 3(a), a larger dot experiences a larger shift in its energy levels due to the

applied field than a smaller one. However, all other parameters being equal, a larger dot also has slightly lower energy at zero field (which is not the case in Fig. 3). Therefore we need a way of increasing the initial energy of the larger dot relative to the smaller one. This could be realised by using layers of different materials (or material concentrations) to alter the band-gap within each dot; however, other methods such as exploiting different dot geometries or applying a local strain should also be explored. Nitride quantum dots offer a promising approach since the strong piezoelectric field allows the external field to shift the energy levels towards each other.

We have also shown that it should be possible to engineer nanostructures such that the off-diagonal Förster interaction between a pair of quantum dots is of the required strength to make it interesting for quantum computation. Once a measurement of this coupling strength is made, the next logical step is to attempt to controllably entangle the excitonic states of two interacting dots, leading on to a demonstration of a simple quantum logic gate such as the controlled-NOT (CNOT). Although on resonance the two qubit states $|01\rangle$ and $|10\rangle$ naturally evolve into maximally entangled states after a time $\pi/(4V_F)$ their initialization requires the inter-dot interaction to be suppressed, and in general the generation of a logic gate such as the CNOT requires single qubit operations on both dots, as well as a controlled interaction.

By switching to a pseudo-spin description of our excitonic qubit we can immediately consider a previously known operation sequence (for example from NMR) for the realization of a CNOT gate. Defining $|\uparrow_z\rangle \equiv |0\rangle$ and $|\downarrow_z\rangle \equiv |1\rangle$, we can see from (26) that the off-diagonal terms can be expressed as:

$$H_F = \frac{V_F}{2} (\sigma_{x_1}\sigma_{x_2} + \sigma_{y_1}\sigma_{y_2}), \quad (43)$$

with

$$\sigma_x = \begin{pmatrix} 0 & 1 \\ 1 & 0 \end{pmatrix} \text{ and } \sigma_y = \begin{pmatrix} 0 & -i \\ i & 0 \end{pmatrix}, \quad (44)$$

being two of the Pauli spin matrices. This XY type Hamiltonian has been studied in the literature for various systems [30], [31] and if the two interacting qubits are left for a time $t = \pi/(2V_F)$ solely under its influence then an iSWAP gate will be executed [32]:

$$\text{iSWAP} = \begin{pmatrix} 1 & 0 & 0 & 0 \\ 0 & 0 & i & 0 \\ 0 & i & 0 & 0 \\ 0 & 0 & 0 & 1 \end{pmatrix}, \quad (45)$$

in the basis $\{|00\rangle, |01\rangle, |10\rangle, |11\rangle\}$. Two iSWAP operations may be concatenated with single qubit operations to form the more familiar CNOT gate:

$$\begin{aligned} \text{CNOT} &= \left(\frac{\pi}{2} \right)_{x_2} \left(\frac{\pi}{2} \right)_{z_2} \left(-\frac{\pi}{2} \right)_{z_1} (\text{iSWAP}) \left(\frac{\pi}{2} \right)_{x_1} \\ &\quad \times (\text{iSWAP}) \left(\frac{\pi}{2} \right)_{z_2}, \quad (46) \end{aligned}$$

where $(\pm\pi/2)_{x/z_{1/2}}$ are single pseudo-spin rotations of $\pm\pi/2$ about the x/z axis of spin 1/2 respectively. Schuch and Siewert [32] have also shown that the CNOT and SWAP operations may be combined when using an XY interaction to produce more efficient quantum circuits.

To perform a gate such as the CNOT outlined above we must be able to control the interaction between our two qubits so that we can effectively switch it off for the duration of the single qubit manipulations. For the case of excitonic qubits, coupled via the Förster mechanism, the most sensible way to proceed is to consider two initially non-resonant quantum dots with negligible energy transfer. Single qubit operations can then be achieved with external laser pulses by inducing Rabi oscillations within each dot [33]. As each dot will have a different excitation energy, we may address them individually by choosing the appropriate frequency. Two periods of free evolution under the interaction Hamiltonian (43) are also required, therefore, we propose that applying a suitably selected detuned pulse to both non-resonant dots will bring them into resonance via the optical Stark effect [34]. We then allow resonant energy transfer to occur for a time $t = \pi/(2V_F)$ producing an iSWAP operation. The detuned pulse is then stopped and single qubit manipulations may be induced as before. We speculate that this all optical approach may have the potential to allow gates to be performed well within the limits set by the nanosecond dephasing times experimentally observed.

Fig. 3(b) provides a nice visualisation of the whole process. We must non-adiabatically switch between the two regimes of zero field, where the dots are effectively uncoupled, and the resonant point where the dots interact. It is our hope that this is achievable through the optical Stark effect, and calculations of its feasibility are ongoing.

To summarise, we have analytically calculated the magnitude of the Förster energy transfer between a pair of generic quantum dots and investigated its effect on their energy level structure. We have proposed a simple experiment which provides a signature of the interaction and an estimate of its strength, and we have also discussed its possible application to quantum information processing.

ACKNOWLEDGEMENT

AN and JHR are supported by EPSRC (JHR as part of the Foresight LINK Award *Nanoelectronics at the Quantum Edge*). BWL thanks St Anne's College for a Junior Research Fellowship. SDB acknowledges support from the E.U. NANOMAGIQ project (Contract no. IST-2001-33186); We thank T. P. Spiller, W. J. Munro, S. C. Benjamin and R. A. Taylor for stimulating discussions.

REFERENCES

- [1] E. Biolatti, I. D'Amico, P. Zanardi, and F. Rossi, "Electro-optical properties of semiconductor quantum dots: Application to quantum information processing," *Phys. Rev. B*, vol. 65, p. 075306, Feb. 2002.
- [2] T. Förster, "Transfer mechanism of electronic excitation," *Disc. Farad. Soc.*, vol. 27, pp. 7–29, 1959.
- [3] C. R. Kagan, C. B. Murray, M. Nirmal, and M. G. Bawendi, "Electronic energy transfer in CdSe quantum dot solids," *Phys. Rev. Lett.*, vol. 76, pp. 1517–1520, Feb. 1996.
- [4] S. A. Crooker, J. A. Hollingsworth, S. Tretiak, and V. I. Klimov, "Spectrally resolved dynamics of energy transfer in quantum-dot assemblies: Towards engineered energy flows in artificial materials," *Phys. Rev. Lett.*, vol. 89, p. 186802, Oct. 2002.
- [5] A. J. Berglund, A. C. Doherty, and H. Mabuchi, "Photon statistics and dynamics of fluorescence resonance energy transfer," *Phys. Rev. Lett.*, vol. 89, p. 068101, July 2002.

- [6] X. C. Hu, T. Ritz, A. Damjanovic, F. Autenrieth, and K. Schulten, "Photosynthetic apparatus of purple bacteria," *Quarterly Reviews of Biophysics*, vol. 35, pp. 1–62, Feb. 2002.
- [7] B. W. Lovett, J. H. Reina, A. Nazir, B. Kothari, and G. A. D. Briggs, "Resonant transfer of excitons and quantum computation," *Phys. Lett. A*, vol. 315, pp. 136–142, June 2003.
- [8] D. L. Dexter, "A theory of sensitized luminescence in solids," *J. Chem. Phys.*, vol. 21, pp. 836–850, 1953.
- [9] B. Krummheuer, V. M. Axt, and T. Kuhn, "Theory of pure dephasing and the resulting absorption line shape in semiconductor quantum dots," *Phys. Rev. B*, vol. 65, p. 195313, May 2002.
- [10] I. D'Amico and F. Rossi, "Field-induced coulomb coupling in semiconductor macroatoms: Application to single-electron quantum devices," *Appl. Phys. Lett.*, vol. 79, pp. 1676–1678, Sept. 2001.
- [11] L. Jacak, P. Hawrylak, and A. Wojs, *Quantum Dots*. Heidelberg: Springer-Verlag, 1998.
- [12] D. J. Eaglesham and M. Cerullo, "Dislocation-free Stranski-Krastanow growth of Ge on Si(100)," *Phys. Rev. Lett.*, vol. 64, pp. 1943–1946, Apr. 1990.
- [13] Q. Xie, A. Madhukar, P. Chen, and N. P. Kobayashi, "Vertically self-organized InAs quantum box islands on GaAs(100)," *Phys. Rev. Lett.*, vol. 75, pp. 2542–2545, Sept. 1995.
- [14] J. Tersoff, C. Teichert, and M. G. Lagally, "Self-organization in growth of quantum dot superlattices," *Phys. Rev. Lett.*, vol. 76, pp. 1675–1678, Mar. 1996.
- [15] M. Califano and P. Harrison, "Approximate methods for the solution of quantum wires and dots: Connection rules between pyramidal, cuboidal, and cubic dots," *J. Appl. Phys.*, vol. 86, pp. 5054–5059, Nov. 1999.
- [16] S. Gangopadhyay and B. R. Nag, "Energy levels in three-dimensional quantum-confinement structures," *Nanotechnology*, vol. 8, pp. 14–17, Mar. 1997.
- [17] M. V. R. Krishna and R. A. Friesner, "Exciton spectra of semiconductor clusters," *Phys. Rev. Lett.*, vol. 67, pp. 629–632, July 1991.
- [18] L. W. Wang and A. Zunger, "Electronic-structure pseudopotential calculations of large (approximate-to-1000 atoms) Si quantum dots," *J. Phys. Chem.*, vol. 98, pp. 2158–2165, Feb. 1994.
- [19] G. Bastard, "Super-lattice band-structure in the envelope-function approximation," *Phys. Rev. B*, vol. 24, pp. 5693–5697, 1981.
- [20] P. Harrison, *Quantum Wells, Wires and Dots*. New York: Wiley, 2001.
- [21] B. W. Lovett, J. H. Reina, A. Nazir, and G. A. D. Briggs. (2003) Optical schemes for quantum computation in quantum dot molecules. [Online]. Available: <http://xxx.lanl.gov/abs/quant-ph/0307021>
- [22] A. Franceschetti, H. Fu, L. W. Wang, and A. Zunger, "Many-body pseudopotential theory of excitons in InP and CdSe quantum dots," *Phys. Rev. B*, vol. 60, pp. 1819–1829, July 1999.
- [23] L. I. Schiff, *Quantum Mechanics*, 2nd ed. McGraw-Hill, 1955.
- [24] K. L. Silverman, R. P. Mirin, S. T. Cundiff, and A. G. Norman, "Direct measurement of polarization resolved transition dipole moment in InGaAs/GaAs quantum dots," *Appl. Phys. Lett.*, vol. 82, pp. 4552–4554, Apr. 2003.
- [25] P. G. Eliseev, H. Li, A. Stintz, G. T. Lin, T. C. Newell, K. J. Malloy, and L. F. Lester, "Transition dipole moment of InAs/InGaAs quantum dots from experiments on ultralow-threshold laser diodes," *Appl. Phys. Lett.*, vol. 77, pp. 262–264, July 2000.
- [26] P. Borri, W. Langbein, S. Schneider, U. Woggon, R. L. Sellin, D. Ouyang, and D. Bimberg, "Ultralong dephasing time in InGaAs quantum dots," *Phys. Rev. Lett.*, vol. 87, p. 157401, Oct. 2001.
- [27] D. Birkedal, K. Leosson, and J. M. Hvam, "Long lived coherence in self-assembled quantum dots," *Phys. Rev. Lett.*, vol. 87, p. 227401, Nov. 2001.
- [28] M. Bayer and A. Forchel, "Temperature dependence of the exciton homogeneous linewidth in $In_{0.60}Ga_{0.40}As$ /GaAs self-assembled quantum dots," *Phys. Rev. B*, vol. 65, p. 41308(R), Jan. 2002.
- [29] Q. Zhang, J. Zhu, X. Ren, H. Li, and T. Wang, "Mismatch and chemical composition analysis of vertical $In_xGa_{1-x}As$ quantum-dot arrays by transmission electron microscopy," *Appl. Phys. Lett.*, vol. 78, pp. 3830–3832, June 2001.
- [30] J. Siewert, R. Fazio, G. M. Palma, and E. Sciacca, "Aspects of qubit dynamics in the presence of leakage," *J. Low Temp. Phys.*, vol. 118, pp. 795–804, Mar. 2000.
- [31] A. Imamoglu, D. D. Awschalom, G. Burkard, D. P. DiVincenzo, D. Loss, M. Sherwin, and A. Small, "Quantum information processing using quantum dot spins and cavity QED," *Phys. Rev. Lett.*, vol. 83, pp. 4204–4207, Nov. 1999.
- [32] N. Schuch and J. Siewert, "Natural two-qubit gate for quantum computation using the XY interaction," *Phys. Rev. A*, vol. 67, p. 032301, Mar. 2003.

- [33] H. Kamada, H. Gotoh, J. Temmyo, T. Takagahara, and H. Ando, "Exciton Rabi oscillation in a single quantum dot," *Phys. Rev. Lett.*, vol. 87, p. 246401, Dec. 2001.
- [34] C. Cohen-Tannoudji, J. Dupont-Roc, and G. Grynberg, *Atom-photon Interactions: Basic Processes and Applications*. New York: Wiley, 1992.